Food and Bioprocess Technology (2022) 15:2776–2788
https://doi.org/10.1007/s11947-022-02917-x

ORIGINAL RESEARCH

Research on the Vegetable Shrinkage During Drying and Characterization and Control Based on LF-NMR

Qing Sun[1,3] · Min Zhang[1,2] · Arun S. Mujumdar[4] · Dongxing Yu[5]

Received: 25 January 2022 / Accepted: 27 September 2022 / Published online: 5 October 2022

Abstract

Shrinkage is a common phenomenon during the drying of fruits and vegetables. The research aimed to study the mechanism of drying shrinkage and investigate the potential use of low-field nuclear magnetic resonance (LF-NMR) for online monitoring changes in shrinkage. The effects of drying parameters (temperature, power, and vacuum) on shrinkage of three types of materials banana (fruit), carrot (vegetable), and *Pleurotus eryngii* (an edible fungus) were studied in the different drying processes of hot air drying (HAD), microwave vacuum drying (MVD), infrared drying (IRD), and infrared freeze-drying (IFD). During drying, material shrinkage mainly occurred in the early and middle drying stages with different characteristics of retention volume and shrinkage equilibrium point of moisture content. The drying shrinkage was significantly related to the change of MC in vacuolar compartment ($p < 0.05$). Reducing the drying time from drying beginning to the LF-NMR $A_{23}/A_{22}(1)$, i.e., when the water content between vacuolar compartment and cytoplasm was equal, was beneficial for reducing shrinkage, and the volume retention rate increased by 39.13%. The shrinkage model of BP-ANN based on LF-NMR had a high prediction accuracy of shrinkage more than 95% and was excellent with the R^2 of 0.9989 and RMSE of 0.0087. The shrinkage control strategy based on LF-NMR provided a reference for the development of artificial intelligence drying equipment.

Keywords Drying · LF-NMR · Shrinkage mechanism · Intelligent control · Fruits and vegetables

Introduction

Drying is an important processing method of fruits and vegetables. New technologies such as microwave vacuum drying (MVD), infrared drying (IRD), microwave freeze-drying (MFD), and infrared freeze-drying (IFD) have made the drying more efficient and energy-saving (Deng et al., 2014; Polat & Izli, 2022; Su et al., 2020; Zeng et al., 2022). Unfortunately, shrinkage has always been an unavoidable defect in all drying methods, which leads to the deterioration of product quality such as a reduction in volume and an increase in hardness (Wang et al., 2018a). Although the shrinkage of freeze-drying products is relatively small, it cannot be ignored (Blahovec et al., 2021; Chen et al., 2021). People put forward higher requirements for product quality and product appearance as one of the important indicators. To solve the problem of shrinkage during drying has become important research in the current food industry.

At present, the researches on drying shrinkage of fruits and vegetables were not thorough enough, mainly focusing on the shrinkage difference of final products after processing (Agudelo-Laverde et al., 2014; Lespinard et al., 2014). There were also fewer studies about shrinkage mechanism, process optimization, and quality improvement (Macedo et al., 2021; Polat & Izli, 2022; Yuyan et al., 2021). Establishing a real-time monitoring method for fruit and vegetable shrinkage

✉ Min Zhang
min@jiangnan.edu.cn; minlichunli@163.com

1 State Key Laboratory of Food Science and Technology, Jiangnan University, Wuxi, Jiangsu 214122, China

2 Jiangsu Province International Joint Laboratory On Fresh Food Smart Processing and Quality Monitoring, Jiangnan University, Wuxi, Jiangsu 214122, China

3 China General Chamber of Commerce Key Laboratory On Fresh Food Processing & Preservation, Jiangnan University, Wuxi, Jiangsu 214122, China

4 Department of Bioresource Engineering, Macdonald Campus, McGill University, Ste. Anne de Bellevue, Quebec H9X 3V9, Canada

5 Shanghao Biotech Co., Ltd., Qingdao, Shandong 266700, China

in the drying process is necessary for realizing shrinkage control and is an indispensable part of the research on fruit and vegetable intelligent drying (Cropotova et al., 2018). Low-field nuclear magnetic resonance (LF-NMR) has made great progress in detection accuracy and cost control and has been widely used in many fields of fruits and vegetables processing, which provides a technical choice for the study of drying shrinkage (Chitrakar et al., 2019; Sun et al., 2019b).

In this research, drying shrinkage of bananas (fruit), carrot (vegetable), and *Pleurotus eryngii* (an edible fungus) during drying by different methods, such as hot air drying (HAD), MVD, IRD, and IFD, was studied from the LF-NMR analysis results with the aim to solve three problems: (1) to explore and improve shrinkage mechanism of fruits and vegetables during drying; (2) to establish the detection method and control strategy of shrinkage of fruits and vegetables during drying based on LF-NMR.

Materials and Methods

Materials and Sample Preparation

The fresh materials of carrot, banana, and *Pleurotus eryngii* for all the experiments were purchased at once from a local supermarket in Wuxi, China, and stored at 4 ± 1 °C. Materials larger than 25 mm in diameter were chosen and cut into cylinders of 25 mm × 25 mm in size by special tool for the pretreatment before drying.

Drying Experiment of Different Materials

Drying by HAD

In HAD, the effect of drying temperature on shrinkage was studied. One hundred grams of pretreated samples (carrot, banana, and *Pleurotus eryngii*) was evenly spread as a single layer in a hot air oven for drying at 50 °C, 60 °C, and 70 °C until the final MC was less than 0.08 g/g w.b., maintaining the airflow rate of 1 m s^{-1}.

Drying by IRD

In IRD, the effect of drying temperature on shrinkage was studied with the emission peak wavelength of 3.0 μm. One hundred grams of pretreated samples (carrot, banana, and *Pleurotus eryngii*) was evenly spread as a single layer in an infrared dryer (Intermediate-wave, Sentteck Co., Ltd., China) for drying at 50 °C, 60 °C, and 70 °C until the final MC was less than 0.08 g/g w.b., maintaining the airflow rate of 1 m s^{-1}.

Drying by MVD

In MVD, the effects of drying temperature, power, and vacuum on the shrinkage were studied. One hundred grams of pretreated samples (carrot, banana, and *Pleurotus eryngii*) was evenly spread as a single layer with a mass load of 0.21 kg/m^2. The effect of drying temperature on shrinkage at 50 °C, 60 °C, and 70 °C was studied until the MC was less than 0.08 g/g w.b., maintaining the power of 200 W and vacuum of 0.01 MPa; the effect of MW power on shrinkage at 100 W, 200 W, 300 W, and 400 W was studied until the MC was less than 0.08 g/g w.b., maintaining the drying temperature of 70 °C and vacuum of 0.01 MPa; and the effect of vacuum on shrinkage at 0.01 MPa, 0.025 MPa, and 0.05 MPa was studied until the MC was less than 0.08 g/g w.b., maintaining the drying temperature of 70 °C and the MW power of 200 W.

Drying by IFD

In IFD, the effects of drying temperature and applied vacuum on the shrinkage were studied. One hundred grams of pretreated samples (carrot, banana, and *Pleurotus eryngii*) was evenly spread in a single layer in the IFD equipment (Changzhou One-Step Drying Equipment Co., Ltd., Changzhou, Jiangsu, China) for drying at 30 °C, 40 °C, and 50 °C until the final MC was less than 0.08 g/g w.b., maintaining the vacuum of 80 Pa; the effect of vacuum on shrinkage at 50 Pa, 130 Pa, and 250 Pa was studied until the MC was less than 0.08 g/g w.b., maintaining the drying temperature of 40 °C.

The Experiment of a Shrinkage Control Strategy Based on LF-NMR

The experiment was performed to evaluate the effect of LF-NMR-based control strategy on the shrinkage of carrots during drying. The carrot was dried by MVD under five methods as follows: (1) drying the carrot to the MC less than 0.08 g/g w.b. at 100 W; (2) the carrot was dried to the A_{23} of 0 at 100 W, then dried to the MC less than 0.08 g/g w.b. at 300 W; (3) the carrot was dried to the A_{23} of 0 at 100 W, then dried to the MC less than 0.08 g/g w.b. at 300 W; (4) drying at 100 W to $A_{23}/A_{22}(50)$, then 300 W to the end; (5) drying at 300 W to the end.

Evaluation Index Measurement Method

Moisture Content

Samples were dried at 105 °C in a hot air oven until the weight difference was less than 2 mg following the Chinese National Standard (GB 5009.3–2016) (China, 2016). The moisture content (MC) was expressed by wet base (Sun et al., 2019a).

Shrinkage

The height and diameter of the sample were measured by digital Vernier calipers (Mitutoyo Corporation, Shanghai, China).

Microstructure

The micromorphology of the sample was evaluated by a scanning electron microscope (Su1510, HITACHI, Japan) with a magnification of 100 × and an optical microscope (Olympus BX43, Tokyo, Japan).

Detection of LF-NMR

The transverse relaxation time (T_2) was measured by an LF-NMR analyzer (MiceoMR 20-030 V-1, Numag Electric Co., Suzhou, China) with Carr-Purcell-Meiboom-Gill pulse sequence (CPMG). SIRT algorithm of the NMR analysis software was applied to transform the CPMG decay curve into T_2 in 100,000 iterative fittings. The detection parameters were set as follows: (1) when MC > 0.3 g/g w.b., repetition time (TR) of 5000 ms; echo time (TE) of 0.6 ms; number of echo (Nech) of 5000; and scan number (NS) of 4; and (2) when MC < 0.3 g/g w.b., TR of 3000 ms; TE of 0.1 ms; Nech of 5000; and NS of 16.

Analysis of Data

Commercial SPSS 16.0 software (SPSS Inc., Chicago, USA) and Origin 2017 (Origin Lab Corporation, Northampton, MA, USA) were used to do the statistical analysis and plotting diagrams. The Unscrambler X (CAMO Software Inc., Oslo, Norway) and MATLAB R2019a (The MathWorks Inc., Natick, MA, USA) were used for modeling with the evaluation index of coefficient of determination (R^2), root mean square error (RMSE), and the accuracy (AC) (Sun et al., 2019a).

$$\mathrm{AC} = \left(1 - \frac{|\exp - \mathrm{pred}|}{\exp}\right) * 100\% \quad (1)$$

where exp is the experimental data, and pred is the predicted data.

Results and Discussion

Theory of Shrinkage in Drying

Prothon and Ahrné (2003) thought that shrinkage went through three stages, namely, cellular shrinkage stage, cell collapse stage, and pore collapse stage, during the drying process except in freeze-drying. However, they did not give a specific classification standard and detail explanation of shrinkage dynamics for each stage. The shrinkage of fruits and vegetables has not been fully explained, but the capillary theory and amorphous viscosity theory are the accepted basic theories at present. According to the capillary theory, there is surface tension at the liquid-gas interface, which acts on the cell wall at the same time. With evaporation, the radius of the semilunar surface decreases, and the surface tension increases, resulting in material shrinkage. Amorphous viscosity theory believes that there is a glass transition temperature in fruits and vegetables. When the temperature of the material is lower than the glass transition temperature, the structure is hard and does not shrink. When the temperature of the material is higher than the glass transition temperature, the molecular movement becomes active, giving higher fluidity, which results in the shrinkage phenomenon. Although two theories explain shrinkage from different perspectives, neither of the two theories can perfectly explain the shrinkage phenomenon in the whole process of drying. For example, Zhengyu and Zhide (1996) illustrated that the surface tension of water in large capillaries is very weak, and its removal does not cause volume change. The capillary theory is more suitable for the pore size less than 0.04 μm. Although the capillary theory can explain pore collapse, it is difficult to explain the cell shrinkage and cell collapse process (Prothon & Ahrné, 2003). Amorphous viscosity theory is mainly used to explain the shrinkage during the freeze-drying process. Collapse and glass transition temperature are interrelated in that significant shrinkage can be noticed during drying only if the temperature of drying is higher than the glass transition temperature of the material at that particular moisture content. It is necessary to improve the characterization theory of shrinkage in the whole drying process of fruits and vegetables. Water in different subcellular organelles is often characterized by different proton relaxation times. The distribution of water proton transverse relaxation times can therefore provide quantitative information about water compartmentation. In addition, the extent to which water diffusion is restricted by membrane and cell wall barriers can also be measured by non-spatially resolved NMR

diffusion techniques. The potential of LF-NMR relaxation in monitoring water compartmentation and drying shrinkage was explored theoretically and experimentally (Hills & Le Floc'h, 1994). Hills et al. (1997) supervised the water change in the apple drying process by LF-NMR with the result that the dried shrinkage mostly resulted from the loss of water from the vacuolar compartment with very little change in the water content of either the cytoplasm or the cell wall compartments.

Study on Shrinkage Mechanism of Typical Fruits and Vegetables During Drying

Study on Shrinkage of Different Materials in HAD

Retention ratio (η) of volume, height, or diameter is an important indicator of the shrinkage degree and is defined as the ratio between the current volume (or length) of the sample and that of the fresh sample, which is usually represented by $\eta = {}^{V}/_{V_0}$ or ${}^{L}/_{L_0}$. The greater the η, the smaller the shrinkage degree. Different materials have different shrinkage characteristics under the influence of different factors such as fiber direction, structure, and composition. Figure 1 shows the results of the volume retention ratio of the three samples after HAD and it was known that different materials had their characteristics in longitudinal and radial shrinkage. The longitudinal and radial shrinkage of carrots was consistent, and the volume retention ratios were all about 50%. Compared with the carrot, the banana had an advantage of radial maintenance with an 11% volume retention ratio higher than the longitudinal volume retention ratio. On the contrary, *Pleurotus eryngii* had a stronger longitudinal maintenance effect. In the process of HAD, carrot, banana, and *Pleurotus eryngii* in the longitudinal and radial

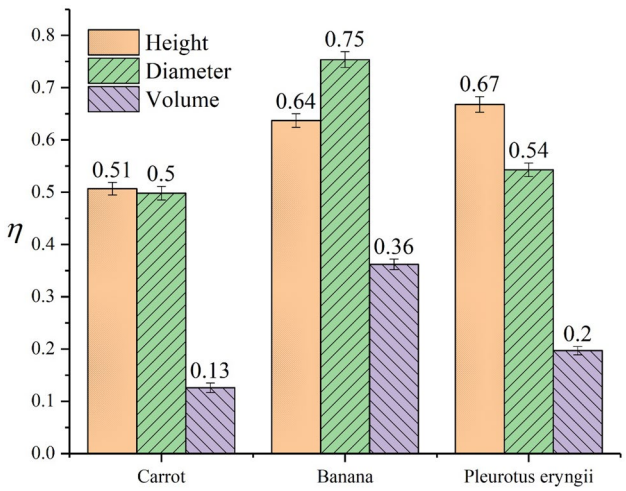

Fig. 1 The shrinkage of materials in HAD

different dimensions had a serious shrinkage. In summary, carrot had a very serious shrinkage, down to 13% of the original volume, while the volume retention ratio of banana was as high as 36%. This might be because carrots being a higher fiber material, heat shrinkage is serious, while the banana has high carbohydrate content and high viscous, providing somehow support during the dehydration process, which is conducive to the maintenance of the spatial structure. Honghong (2012) found that papaya with high maturity was less prone to shrinkage than papaya with low maturity due to its high sugar content. Lozano et al. (1983) found that the volume retention ratio of carrot, pear, potato, and garlic was from 10 to 30%. The higher the starch content in the sample, the larger the retention volume and the smaller the shrinkage so that the material finally has a good volume retention ratio. The shrinkage of fruits and vegetables material has different shrinkage characteristics due to its different components.

Figure 2 shows the relationship between volume retention ratio and moisture content (MC) during the process of HAD. With the drying process, the MC decreased gradually, and the material showed the law of rapid shrinkage at first, then slowly change in shrinkage. There was an obvious inflection point of shrinkage in MC variation (Blahovec et al., 2021). There was a significant linear correlation between shrinkage and MC on both sides of the inflection point. As can be seen from Fig. 2a, when shrinkage was at the high MC stage, *Pleurotus eryngii* and carrot had a more similar shrinkage pattern. However, when MC was low, the volume retention ratio of banana and *Pleurotus eryngii* had a smaller change, while that of carrot lasted until the end of drying. There was a more obvious inflection point in banana and *Pleurotus eryngii*, which were 0.5 g/g (w.b.) and 0.7 g/g (w.b.) of MC, respectively, while carrot had a wide inflection in the range of 0.5–0.8 g/g (w.b.) of MC. Shrinkage is the result of radial shrinkage and longitudinal shrinkage. It can be seen from Fig. 2b and c that there were certain differences in radial and longitudinal shrinkage laws for different materials. As shown in Fig. 2b of longitudinal shrinkage, banana shriveled rapidly at the beginning, and then at a slower rate, *Pleurotus eryngii* shriveled rapidly and then stabilized, while carrots slowly decreased in height throughout the drying process. The radial shrinkage of carrot was the most serious, *Pleurotus eryngii* was the second most, and banana was the least at the same MC level.

The shrinkage of the three types of materials showed obvious consistency, that is, at the beginning of drying, the volume retention ratio reduced rapidly and showed a strong linear relationship with MC, and then slowly or tended to be stable. This was because, at the beginning of drying of fruits and vegetables, water evaporated and dissipated, and shrinkage of cells and large capillaries made up for space loss. Therefore, volume shrinkage is related to water loss.

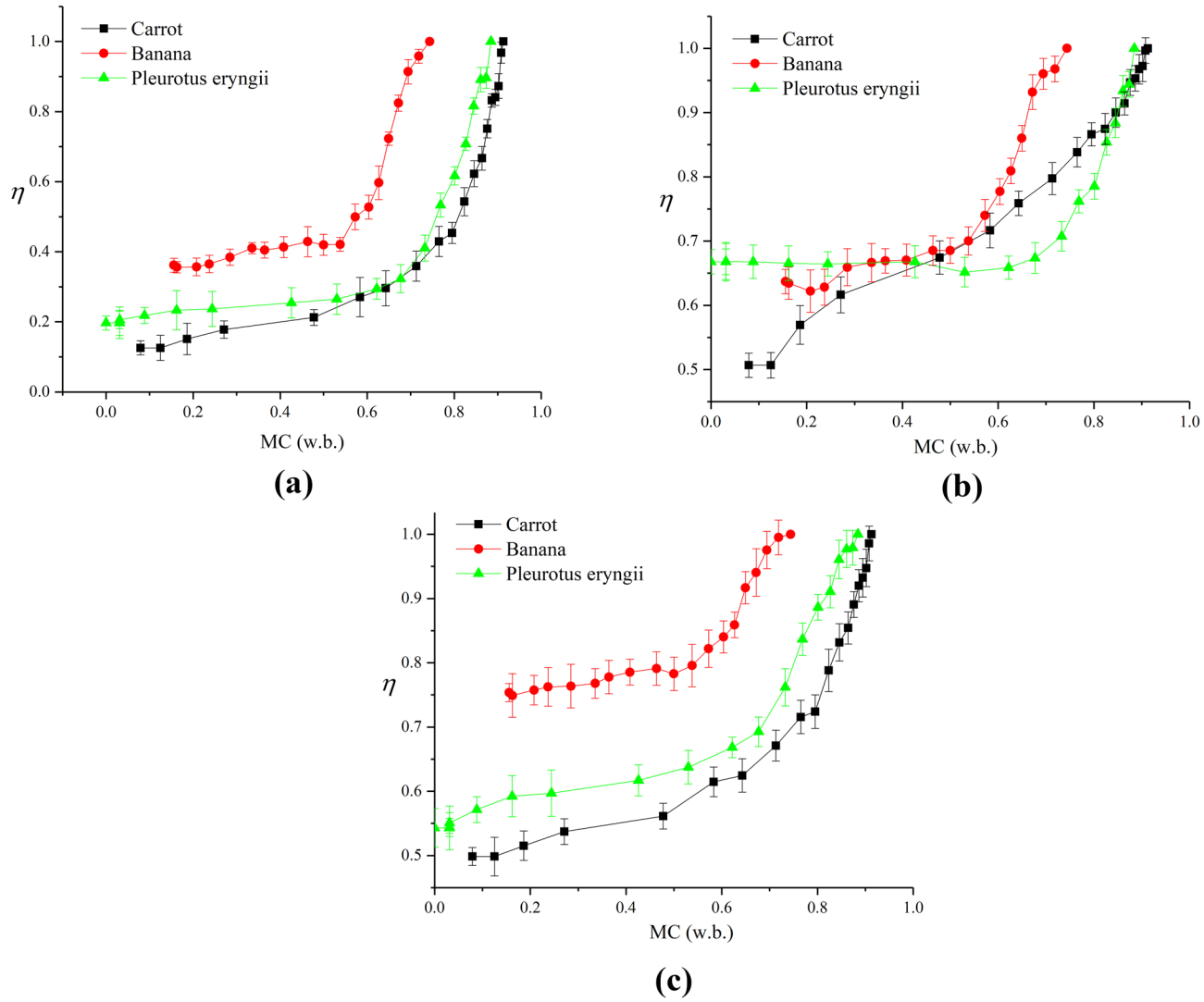

Fig. 2 Retention ratio of materials with moisture content: **a** volume, **b** height, and **c** diameter

Moreover, the internal and external pressure difference of materials is also an important power source of shrinkage at the beginning (Jianrong et al., 2019; Yue, 2020). With the loss of water and the increase of material temperature, there are two types of water migration in the material: liquid phase infiltration and gas transport. As the water in the large capillary disappears, the internal and external pressure difference force weakens, and the main force in the small capillary gradually increases, that is, the surface tension becomes the main factor affecting volume. With the further decrease of water content, the glass temperature of the material gradually increases, the anti-shrinkage ability increases, and the shrinkage slows down or stops. Lili et al. (2016) found that at low MC, the material continuously transforms from a high elastic state to a glass state, and its rigidity increases, which counteracts part of the capillary force and hinders further shrinkage.

Zhen (2019) found that in the heat pump drying of *Pleurotus eryngii*, the volume retention ratio presented a linear relationship with water content at the early drying stage, and the change of volume shrinkage was no longer obvious when the MC was reduced to 60%. The same phenomenon occurred in the process of dehydration and drying of banana, mango, pineapple, potato, and lemon (Jianrong et al., 2019; Wang et al., 2018b). But the inflection of MC tending to be stable was lower than that in this study, which might be the result of the many effects of different materials, different drying methods, and drying processes. It is also an interesting scientific question to explore the key points that affect the shrinkage transition. Gongnian et al. (2005) studied a vacuum freeze-drying combined with a hot air drying method based on the characteristics that shrinkage concentrated in the early drying stage, which played a positive role in reducing shrinkage.

As another indicator of the shrinkage degree, shrinkage rate (ψ) was used to express the speed of shrinkage and was often represented by $\psi = \frac{V_{t_i} - V_{t_j}}{t_i - t_j}$ or $\frac{L_{t_i} - L_{t_j}}{t_i - t_j}$. Figure S1 shows clearly the relationship between shrinkage rate and MC during the HAD process. The maximum shrinkage rate of carrot was 38.50 mm^3/min when the MC was 0.90 g/g w.b. The peak volume shrinkage rate of *Pleurotus eryngii* and carrot was similar, that is, the shrinkage rate increased sharply to the maximum at the beginning of drying, and reached the maximum shrinkage rate of 40.16 mm^3/min when the MC of *Pleurotus eryngii* was 0.87 g/g w.b. However, the difference of shrinkage rate between *Pleurotus eryngii* and carrot was that after the peak of volume shrinkage, the shrinkage rate of carrot decreased slowly, while *Pleurotus eryngii* decreased quickly. Banana showed a trend of slowly increasing and then decreasing shrinkage rate, and the MC at the highest shrinkage rate was relatively low (0.65 g/g w.b.). The radial and longitudinal shrinkage rates were all similar, that is, the maximum longitudinal and transverse shrinkage rates were reached at the same MC.

Effect of Drying Methods on Material Shrinkage

The effect of four kinds of typical drying methods (HAD, IRD, MVD, and IFD) on material shrinkage was studied. To facilitate the intuitive explanation, Figure S2 shows the real photos and SEM of dried carrot at three different levels of MC (high, medium, and low MC). As can be seen, compared with fresh carrot, the shrinkage of IFD carrot was little with a light texture and white color. Pikal and Shah (1990) believed that shrinkage happened only under drying temperature higher than the glass transition temperature of the material being dried in FID. While MC was a more important factor affecting shrinkage in HAD, IRD, and MVD, viz., the shrinkage became more severe at lower MC. The volume retention ratio of carrot changed greatly at high MC and tended to be stable in the late drying stage, which further proved that the main stage of shrinkage occurred during the evaporation of water from vacuolar compartment. The carrots dried by IRD and HAD were similar in appearance, with serious shrinkage, dark color, and hard texture. The carrot dried by MVD was lighter in color and larger in retention volume. These results were attributable to that, with higher drying efficiency and shorter drying time, the volumetric heating of MVD avoids great temperature fluctuations and better preserves the structure and porosity in tissues (Talens et al., 2017; Conte et al., 2019).

The internal structure of the carrot was also studied by scanning electron microscopy (SEM). The carrot treated by HAD and IRD had similar structural characteristics, with dense texture, high hardness, and severe drying shrinkage. The carrot treated by MVD had certain cracks but had larger pores. There was a relatively complete cellular structure with good homogeneity in carrot of IFD drying. Jingjing et al. (2011) also found there was better pore structure in jujube dried by microwave drying and freeze-drying. In the microwave drying process, the high intensity of microwave energy makes the water inside the carrot produce a certain degree of gasification, and the swelling pressure of water vapor weakens the effect of external pressure on the material to a certain extent. Therefore, the carrot treated by MVD had a large retention volume. Compared with HAD and IRD, Miaoqing (2019) also found that *Pleurotus eryngii* treated by MVD had a larger retention volume. Zongbo (2016) believed that microwave expansion was the main force for improving the retention volume (Zielinska et al., 2017).

Figure S3 shows the effect of the four drying methods on the radial shrinkage and longitudinal shrinkage of three kinds of materials respectively. It can be seen that the shrinkage of both longitudinal and radial directions of all materials dried by IFD was not obvious; this is because, during the cryosublimation process, the material temperature is always below the disintegration temperature to maintain high support strength. In addition, gaseous water does not produce serious surface tension on the capillary, and the material finally retains a relatively complete cell structure and small shrinkage. Compared with HAD, MVD and IRD had a smaller degree of longitudinal shrinkage. The effect of MVD on the longitudinal retention ratio of carrot and banana was significantly increased by 48.10% and 37.72%, respectively, while the effect on the longitudinal shrinkage of *Pleurotus eryngii* was not significant ($p > 0.05$). Conte et al. (2019) found that compared with HAD, the retention ratio of apple slices dried by microwave increased by more than 50%, which had an obvious effect. Koç et al. (2008) studied the shrinkage regularity of quince in freeze-drying (FD), IFD, fluidized bed drying (FBD), and HAD, and in the process of osmosis pretreatment, hot air drying, and found the material dried by FD had minimum shrinkage and retention volume up to 90%. Compared with HAD, IRD, FBD, and osmosis pretreatment could improve the retention volume.

Effect of Drying Temperature on Material Shrinkage

The increase of drying temperature led to the aggravation of material shrinkage as shown in Fig. S4a, which might be because the increase of temperature accelerates water diffusion and rapid evaporation, resulting in the increase of internal and external pressure difference of material in a short time, so the shrinkage is obvious (Vallespir et al., 2019). Xueyuan et al. (2015) studied the volume retention ratio of apples during medium-short-wave IRD and found that the higher the drying temperature, the smaller the volume retention ratio. Compared with the temperature at 95 °C, the volume retention ratio of potato (Yue, 2020) and garlic (Abbasi

et al., 2011) induced with the increase of temperature during drying. In the frying dehydration method, the volume retention ratio of *Pleurotus eryngii* increased by 17.5% at 75 °C (Zhengxiang, 2016). Haonan (2020) proposed that the drying temperature difference between the sample and the glass transition temperature of materials was also an important cause of shrinkage. In heat pump drying of jujube chips, the greater the temperature difference, the smaller the volume retention ratio. Karathanos (1993) proposed the same shrinkage theory based on the temperature difference. However, the lower the drying temperature is not the better; too long drying process would increase the overall effect of shrinkage factors, resulting in increased shrinkage (Pikal & Shah, 1990). Lili et al. (2016) found that under too low drying intensity, the internal water penetration of carrot was slower and the cell wall deformation was larger. Qinghui et al. (2017) found that in the shrinkage experiment of ginkgo biloba by HAD, the volume retention ratio first increased and then decreased with the increase of drying temperature.

Effect of Vacuum on Material Shrinkage

Figure S4b shows the relationship between vacuum and volume retention ratio in MVD and IFD. It can be seen that the material volume retention ratio increased with the decrease of pressure, that is to say, improving the vacuum degree of the drying environment is beneficial to the maintenance of product volume. This is because in the process of water evaporation, the improvement of vacuum on the one hand can reduce the effect of pressure difference on the material, at the same time can improve the drying rate, and shorten the shrinkage time. In IFD, the low vacuum can also reduce the triple point of water and is beneficial to prevent the formation of liquid water, which is the common cause of shrinkage in IFD.

Effect of Microwave Power on Material Shrinkage

Figure S5 shows the effect of microwave intensity on physical shrinkage, and it can be seen that the volume retention ratio increased first and then decreased with the increase of microwave power intensity. When the microwave power increased from 100 to 300 W, the retained volume of carrot increased by 29.57%. When the microwave intensity continued to increase, the material shrinkage is serious, and its volume decreased. This may be because the high intensity of processing conditions destroyed the cellular structure of the carrot, resulting in material collapse. Miaomiao et al. (2020) believed that microwave made water vaporize into steam in a short time, and the volume expanded instantly at a speed greater than its diffusion speed, which expanded the spatial structure of the material and formed a large porosity channel. Yuyan et al. (2021) found persimmon shrinkage obviously in drying condition of low microwave power and, with the increase of microwave power, persimmon fruit expansion of internal organization with large convex on the material surface. When power continues to be increased, a big difference of vapor pressure made the moisture in the form of liquid water inside the persimmon fruit surface of direct precipitation, causing the product quality very poor, and shrivel. Lili et al. (2016) found in the shrinkage experiment of carrot dried by infrared radiation that with the increase of drying intensity, the volume retention ratio of carrot showed a trend of first increasing and then decreasing. The material picture shows the influence of microwave intensity on the internal structure of the material in a more intuitive and detailed way as shown in Fig. S5. The internal structure of carrot dried at low power was dense and complete and, with the increase of microwave power, the pore gradually increased and became larger. When the microwave power was 300 W, the material porosity reached the maximum. As the microwave intensity continued to increase, the pores fused into large airways, the rigid structure was destroyed, and the tissue collapsed seriously.

Establishment of Fruits and Vegetables Drying Shrinkage Model Based on LF-NMR

LF-NMR is a potential nondestructive detection method to monitor the distribution and amount of water proton in different subcellular compartments based on different and characteristic water proton transverse relaxation times (T_2) determined mainly by fast proton exchange between water and exchangeable protons on biopolymers and dissolved metabolites (Hills & Le Floc'h, 1994). The shortest transverse relaxation time T_{21} could be assigned to water associated with cell walls, and would be the result of chemical exchange effect due to fast proton exchange between water and hydroxyl protons on the rigid cell wall polysaccharides (pectin, cellulose, hemicellulose). The intermediate relaxation time T_{22} could distinguish water residing in the cytoplasm and could be explained on the basis of a proton chemical exchange between water and proteins of the cytoskeleton and enzymes and the high viscosity of the cytosol. The highest relaxation time T_{23} could be attributed to water located within the vacuole, arising from the chemical exchange with sugars and other low weight compounds that constitute the dilute solution of the sap (Nieto et al., 2013). According to the distribution of water, T_2 of carrot, banana, and *Pleurotus eryngii* can be divided into T_{20}, 0.1–1 ms; T_{21}, 1–10 ms; T_{22}, 10–100 ms; and T_{23}, 100–1000 ms (Sun et al., 2019c). The corresponding total signal amplitudes of different water were A_{20}, A_{21}, A_{22}, and A_{23}, and the total signal amplitude of all water was A_{Total} (Lv et al., 2017).

Data Analysis of LF-NMR

As shown in Fig. S6 for the T_2 distribution of the three fresh materials, the T_{23} of *Pleurotus eryngii*, carrot, and banana

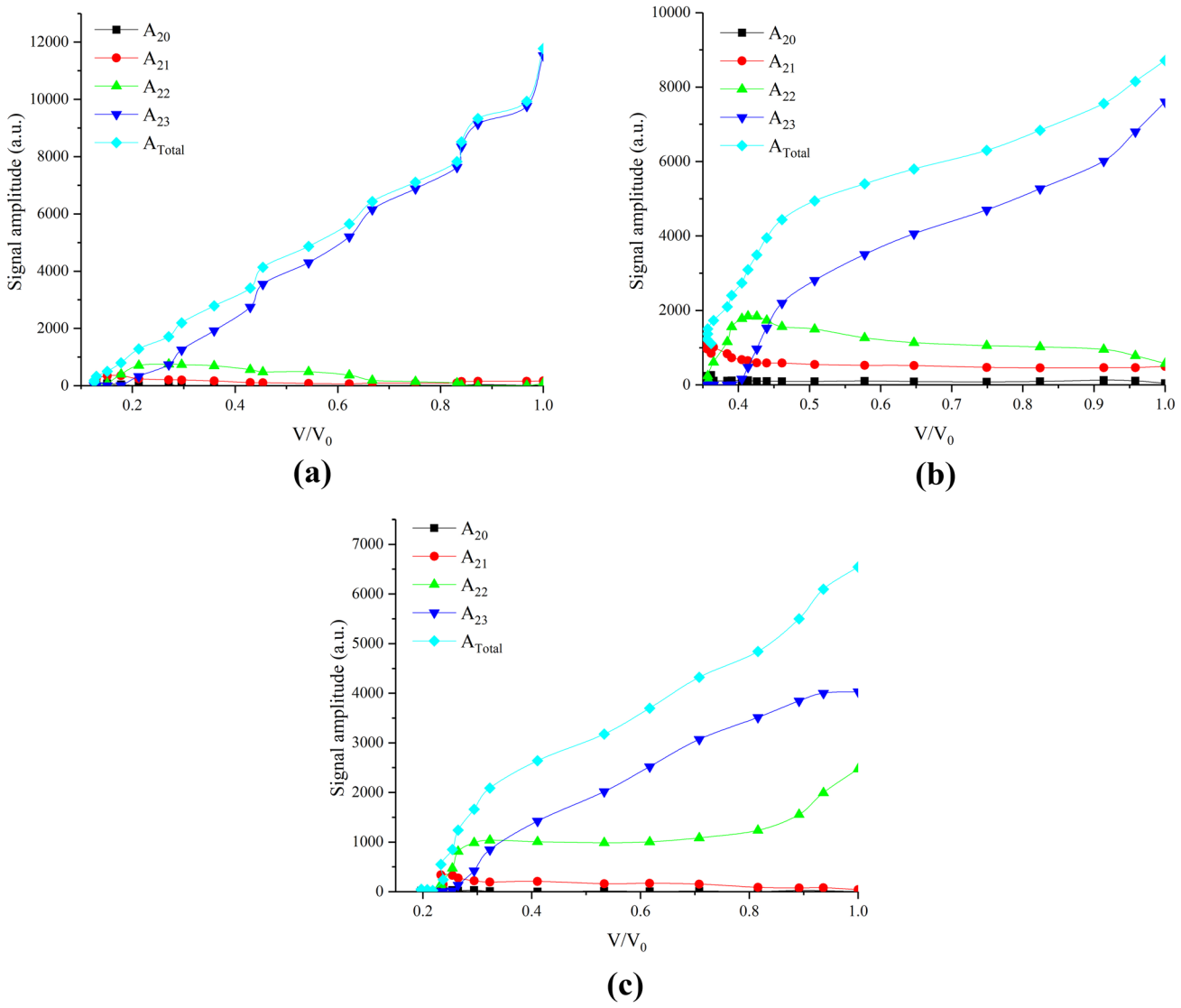

Fig. 3 The LF-NMR signals of different materials with volume retention ratio: **a** carrot **b** banana, and **c** *Pleurotus eryngii*

were 310, 357, and 580 ms respectively. It was clear that the water from vacuolar in banana was more diffuse and exchangeable. One more interesting thing was that the T_2 distribution of *Pleurotus eryngii* was multiexponential with two main relaxation components. As to the amount of water proton, different materials had different water states. Most of water came from vacuolar, accounting for 87.46% in banana, 68.77% in *Pleurotus eryngii*, and 86.32% in carrot. Due to the higher content of protein, A_{22} accounted for a greater proportion (28.80%) in *Pleurotus eryngii*. The T_2 distribution of carrot during HAD was also studied as shown in Fig. S7. As the drying time increased, drying is seen to result in a reduction in the peak area of the vacuolar compartment relative to the other compartments from 11,526.84 to 4.05 a.u. and a gradual shift in the vacuolar peak to shorter T_2, which can be explained in terms of two exchange mechanisms: chemical exchange and diffusive exchange. Chemical exchange gives rise to a dispersion of T_2 and diffusive exchange gives rise to multiexponential behavior (Hills et al., 1990). For example, in the later stage of drying, the ingredient of macromolecular materials (such as enzymes, proteins) enhances the ability of base materials to the water (Sun et al., 2019c).

Figure 3 shows the relationship between volume retention ratio and MC during the drying. As can be seen, the water content from cell wall compartments in the three materials was small, the water content from vacuolar compartment in carrot was the highest, the proportion of water from cytoplasm in banana increased, and *Pleurotus eryngii* had a higher proportion of water from cytoplasm than carrot and banana, which explains why carrot shriveled the most seriously in the three materials. At the same time, the water in carrot is mostly from vacuolar compartment, so the change

Table 1 The MCs of shrinkage inflection point and A_{23}/A_{22} (1) in different drying methods

	HAD			IRD			MVD		
	Carrot	**Banana**	***Pleurotus eryngii***	**Carrot**	**Banana**	***Pleurotus eryngii***	**Carrot**	**Banana**	***Pleurotus eryngii***
Key η point	0.55 ± 0.11	0.51 ± 0.10	0.65 ± 0.13	0.55 ± 0.10	0.50 ± 0.10	0.58 ± 0.12	0.53 ± 0.12	0.45 ± 0.08	0.53 ± 0.10
$A_{23}/A_{22} = 1$	0.60 ± 0.12	0.51 ± 0.11	0.70 ± 0.10	0.58 ± 0.13	0.55 ± 0.10	0.65 ± 0.13	0.57 ± 0.14	0.50 ± 0.12	0.60 ± 0.12

of water from vacuolar compartment in the drying process is similar to the change of total water. Although banana and *Pleurotus eryngii* had more water from cytoplasm, resulting in a certain difference in the content of water from vacuolar compartment and cytoplasm in the drying process, the trend of change was the same, namely, with the drying process, the material gradually shrank, and the total water and vacuolar water content continued to decrease. During the whole drying process, the water from cytoplasm of carrot and banana firstly increased and then decreased, which was because with the decrease of the vacuolar water, the carbohydrate concentration increased, prompting partial vacuolar water to be converted into cytoplasm water (Sun et al., 2019c). The change rule of water from cytoplasm of *Pleurotus eryngii* was different from that of carrot and banana. The cytoplasm water was converted to vacuolar water at the early drying stage, which was also the reason why the change of water content from vacuolar compartment of *Pleurotus eryngii* was not significant at the early drying stage.

Consistent from the "Study on Shrinkage of Different Materials in HAD" section with regard to changes in volume retention ratio and MC, Fig. 3 also shows that the key points of LF-NMR signals appeared at the inflection point of dry shrinkage, that is, after the volume retention ratio of carrot, banana, and *Pleurotus eryngii* tended to be stable, the material volume did not change much, although the LF-NMR signals still decreased. Interesting but important information was found here that at the inflection point of volume retention ratio, the signal amplitude of A_{23} was equivalent to A_{total} ($A_{23}/A_{total} = 1$). Therefore, it was guessed that when the signal amplitude of water from vacuolar compartment and that of water from cytoplasm were equivalent, it was the key point for the transition of shrinkage from osmotic pressure difference to surface tension caused by small capillaries.

To verify this conjecture, the inflection points of shrinkage and the LF-NMR signal point of $A_{23}/A_{total} = 1$ of the three kinds of samples dried by different methods were studied, and the results are shown in Table 1. As can be seen from the table, the MC at the signal of $A_{23}/A_{22} = 1$ was very similar to the MC at the volume inflection point, and the deviation was between 4 and 13% on the whole. It can also be seen that LF-NMR had higher accuracy for the processing method with softer action intensity. The accuracy deviation of IRD was between 5 and 12% and that of MVD was 7 and 13%. Therefore, the signal critical control point of $A_{23}/A_{total} = 1$ has practical significance for process guidance.

Volume shrinkage ratio (ζ) represents the relative dimensional change in volume and is often represented by $\Delta V/V_0$. Figure S8 shows the relationship between material shrinkage ratio and signal change ratio of A_{23} and A_{Total}. When the value is on the line, it indicates that the shrinkage ratio is equal to the water loss rate; when it is above the line, it indicates that the water loss rate is greater than the volume shrinkage rate; and when it is below the line, it indicates that the water loss rate is less than the volume shrinkage rate. As shown in Fig. S8, compared with the change of water from vacuolar compartment in the three kinds of materials, the correlation between the change of total water and the volume shrinkage was stronger. The signal change of A_{23} in carrot and banana was over the bisector, suggesting that the decrease of the water from vacuolar compartment reducing rate was greater than the material volume shrinkage rate; this is because the water loss from vacuolar compartment in the two kinds of material is mainly divided into two parts, one is the volume shrinkage, the other is converted into cytoplasm water; Fig. S8 can be very good to prove the argument. However, the change ratio of A_{23} in *Pleurotus eryngii* was below the bisector line, which indicated that in addition to the loss of water from vacuolar compartment, the loss of water from cytoplasm was also the main factor of volume shrinkage, which made the contribution as high as 50%. Therefore, the causes of drying volume shrinkage were different with different material properties. The change ratio of A_{Total} content in banana and *Pleurotus eryngii* was all above the bisector line in the late drying stage, and the phenomenon of abrupt increase appeared in banana and *Pleurotus eryngii*, which was because the change of material shrinkage decreased and the volume tended to be stable in the late drying period, and the rate of water loss was much higher than the rate of volume change.

Correlation Analysis of Signal and Shrinkage

At present, one of the important problems of intelligent drying is the lack of technical means of online monitoring of material state. It is very important to establish an effective and accurate monitoring method for intelligent equipment manufacturing. LF-NMR can reflect the shrinkage change during the drying process of fruits and vegetables. The

quantitative model of volume shrinkage based on the signal of LF-NMR was studied, providing ideas for precise control of intelligent drying. Figure 4 shows the relationship between the volume retention ratio (η) and the signal of A_{23} and A_{Total} during banana drying. The data of the whole drying process and the data of high MC were analyzed by linear fitting respectively. It is known that the correlation coefficient (R^2) between volume retention ratio and A_{Total} and A_{23} was 0.9187 and 0.967 respectively in the linear fitting of whole drying data and 0.9814 and 0.9807 respectively in the linear fitting of high MC. The result showed that in high MC, the A_{Total} was more suitable for the numerical modeling of volume shrinkage, which is because the water from vacuolar compartment is involved in the change of the water from cytoplasm, which leads to a slight deviation from the value of the volume shrinkage. To verify the law, the correlation of other drying patterns was studied and the results are shown in Table S1. The same conclusion was that the volume shrinkage model based on the signal of LF-NMR should be built in two parts. The A_{23} was adopted in the high MC, and A_{Total} was adopted in the low MC stage, which was positive for the accuracy of the model.

To improve the accuracy of the model, the model of volume shrinkage based on multiple parameters such as drying method, types of material, A_{20}, A_{21}, A_{22}, A_{23}, and A_{Total} was also studied. The result showed that the additional information of multiple parameters significantly improves the R^2 and accuracy of the model. In later model builds, the default is full information as the input parameters.

Analysis of Shrinkage Model Based on Signals of LF-NMR

Multiple linear regression (MLR) method, support vector machine (SVM) method, partial least square (PLS) method, and back propagation artificial neural network (BP-ANN) are the mainstream and excellent numerical fitting models. To achieve accurate prediction and control of the drying process, volume shrinkage models based on these four methods were evaluated with R^2 and root mean square error (RMSE). In all models, the inputs were drying method (HAD, IRD, and MVD), type of material (carrot, banana, and *Pleurotus eryngii*), A_{20}, A_{21}, A_{22}, A_{23}, and A_{Total} and the output was the volume retention ratio. A total of 1230 groups of data were collected, including 540 groups of HAD data, 480 groups of IRD data, and 210 groups of MVD data. The performance comparison of different models is shown in Table S2, in which the BP-ANN model showed the best performance with the R^2 of 0.9989 and RMSE of 0.0087. The main parameters of the optimal BP-ANN model were the topology of 7–20-1, transfer function of tansig and purelin, and training function of trainlm. In order to test the actual prediction of shrinkage ratio, 24 groups of experimental data (8 groups of data for each of three different materials) were used for the evaluation of the result. The test result in Fig. S9 showed that the residual difference between the predicted value and the actual value was mainly concentrated in the range of −0.03–0.05 with the R^2 of 0.9886 and RMSE of 0.0217. The prediction accuracy (AC) of the model was different in the whole drying process. At the beginning drying stage, that is, with high moisture content, the model had a

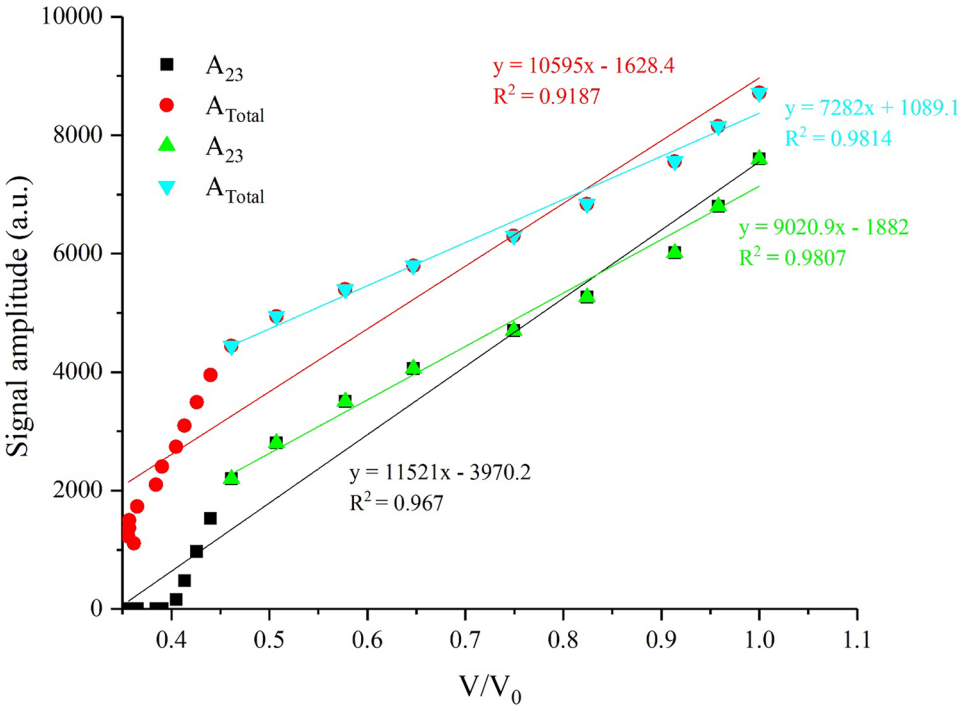

Fig. 4 Linear fitting between volume retention ratio and signal

Table 2 Results of a shrinkage control strategy based on LF-NMR in drying

Experiment	Detected shrinkage (η)	Predicted shrinkage (η)	Accuracy	Drying time (min)
Drying at 100 W to the end	0.23	0.26	86.96%	100
Drying at 100 W to A_{23}/A_{22} (0), then 300 W to the end	0.25	0.31	76%	90
Drying at 100 W to A_{23}/A_{22} (1), then 300 W to the end	0.27	0.33	77.78%	65
Drying at 100 W to A_{23}/A_{22} (50), then 300 W to the end	0.32	0.41	75%	47
Drying at 300 W to the end	0.33	0.38	87.88%	40

higher prediction accuracy (AC > 95%). In the late drying stage, there are more factors affecting the shrinkage besides the water and the AC decreased to 80%. However, the model meets the drying needs of actual production and has great potential in the intelligent control strategy.

Application of Shrinkage Control Strategy Based on LF-NMR in Drying

It is known from the "Data Analysis of LF-NMR" section that the ratio value of A_{23}/A_{22} is the key point of shrinkage change during drying, based on which the application of shrinkage control strategy during the MVD process of carrot was studied in this part. In the range of 100–400 W microwave power, the volume retention ratio of the dried product increased first and then decreased with the increase of microwave power, so 100 W and 300 W were selected as the control parameter. During the drying process, the volume retention ratio decreased rapidly and then the material volume tended to be stable when A_{23}/A_{22} reached 1. Therefore, three signal points of A_{23}/A_{22} (50) (A_{23}/A_{22} = 50) of high MC, A_{23}/A_{22} (1) of volume shrinkage stable inflection point, and A_{23}/A_{22} (0) of low MC were selected. Five experiments were designed respectively as follows: (1) drying at 100 W to the end; (2) drying at 100 W to A_{23}/A_{22} (0), then 300 W to the end; (3) drying at 100 W to A_{23}/A_{22}(1), then 300 W to the end; (4) drying at 100 W to A_{23}/A_{22} (50), then 300 W to the end. At the beginning of drying, the shrinkage model based on LF-NMR was used to detect the state of materials online in real time, and the microwave power was adjusted according to the experimental design when drying to the predetermined point of A_{23}/A_{22}. The dried shrinkage ratio, the shrinkage ratio predicted by LF-NMR model, shrinkage accuracy (AC), and drying time were taken as experimental evaluation indexes, and the results are shown in Table 2.

The accuracy of carrot dried in 100 W and 300 W set power during drying was 86.96% and 87.88%, respectively, while the prediction accuracy of variable power drying was 76%, 77.78%, and 75%, respectively. It can be seen that the change of drying parameters during the drying process has a certain influence on the model prediction accuracy. Other drying factors should also be considered to improve the performance of the model. Compared with fixed 100 W microwave power drying process, the volume of materials increased by 39.13%, 17.39%, and 8.69% at A_{23}/A_{22} (50), A_{23}/A_{22} (1), and A_{23}/A_{22} (0), respectively. It can be seen that the enhancement of drying power is more beneficial to the retention of volume at the stage of high MC, while the change of microwave power has no obvious effect on volume improvement during the low MC stage. As the critical point of drying parameter adjustment, A_{23}/A_{22} (1) is of great significance for process control and improvement of material appearance quality. Therefore, LF-NMR is feasible in the monitoring and optimization of material volume during fruits and vegetables drying and has potential application value for the development of intelligent equipment.

Conclusion

In this research, three typical materials, namely banana (fruit), carrot (vegetable), and *Pleurotus eryngii* (an edible fungus), were used in different drying processes, including HAD, MVD, IRD, and IFD, to analyze the effects of drying parameters (temperature, power, and vacuum) on shrinkage. The shrinkage mainly occurred in the early drying stage and then tended to stabilize. Different materials and drying methods had different effects on the longitudinal and radial shrinkage. Banana had the best volume retention ratio of 36% among the three samples after drying and IFD was the best way to dry fruits and vegetables with less loss of volume appearance. Appropriate microwave treatment was found to increase volume retention of fruits and vegetables, especially for materials with high starch content. Low temperature and pressure environments were found favorable for weakening drying shrinkage. LF-NMR was used to monitor the shrinkage change during process and found that there was a significant linear relationship between shrinkage and water loss at high moisture content. The signal of A_{23}/A_{22} (1) was the key point for the transition of dry shrinkage from osmotic pressure difference to surface tension caused by small capillaries. Full signal information (A_{20}, A_{21}, A_{22}, A_{23}, and A_{Total}) can greatly improve the prediction performance of drying shrinkage model compared with just using A_{23} or A_{Total}. Four shrinkage

models, namely MLR, SVM, PLS, and BP-ANN, based on information of LF-NMR were studied, and the best and the most optimized BP-ANN model had good performance with the R^2 of 0.9989, RMSE of 0.0087, and higher prediction accuracy (AC > 95%). The shrinkage control strategy, based on LF-NMR, appears to be effective and has potential application value for the development of intelligent equipment.

Supplementary Information The online version contains supplementary material available at https://doi.org/10.1007/s11947-022-02917-x.

Funding We acknowledge the financial support from the National First-class Discipline Program of Food Science and Technology (no. JUFSTR20180205), Jiangsu Key Laboratory of Advanced Food Manufacturing Equipment & Technology (nos. FMZ202003 and FM-2019–03), Postgraduate Research & Practice Innovation Program of Jiangsu Province (KYCX19-1816), and Special funds for Taishan Industry Leading Talents Project, all of which enabled us to carry out this study.

Data Availability The data are available from the corresponding author upon suitable request.

Declarations

Conflict of Interest The authors declare no competing interests.

References

Abbasi, S., Mousavi, S. M., & Mohebbi, M. (2011). Investigation of changes in physical properties and microstructure and mathematical modeling of shrinkage of onion during hot air drying. *Iranian Food Science and Technology, 7*, 92–98.

Agudelo-Laverde, L. M., Schebor, C., & Buera, M. D. P. (2014). Evaluation of structural shrinkage on freeze-dried fruits by image analysis: Effect of relative humidity and heat treatment. *Food and Bioprocess Technology, 7*(9), 2618–2626.

Blahovec, J., Kouřím, P., & Lebovka, N. (2021). Volumetric shrinkage and Poisson's ratio of carrot treated by pulse electric fields. *Food and Bioprocess Technology, 14*(11), 2134–2145.

Chen, F., Zhang, M., Devahastin, S., & Yu, D. (2021). Comparative evaluation of the properties of deep-frozen blueberries dried by vacuum infrared freeze drying with the use of CO_2 laser perforation, ultrasound, and freezing–thawing as pretreatments. *Food and Bioprocess Technology, 14*(10), 1805–1816.

China, National Health and Family Planning Commission. (2016). Determination of moisture in food. *Chinese National Standard,* GB5009.3–2016: 1–8.

Chitrakar, B., Zhang, M., & Bhandari, B. (2019). Novel intelligent detection of safer water activity by LF-NMR spectra for selected fruits and vegetables during drying. *Food and Bioprocess Technology, 12*(7), 1093–1101.

Conte, P., Cuccurullo, G., Metallo, A., Micalizzi, A., Cinquanta, L., & Corona, O. (2019). Comparing different processing methods in apple slice drying. Part 2 solid state fast field cycling ^{1}H-NMR relaxation properties, shrinkage and changes in volatile compounds. *Biosystems Engineering, 188*, 345–354.

Cropotova, J., Mozuraityte, R., Standal, I. B., & Rustad, T. (2018). A non-invasive approach to assess texture changes in sous-vide cooked Atlantic mackerel during chilled storage by fluorescence imaging. *Food Control, 92*, 216–224.

Deng, Y., Wang, Y., Yue, J., Liu, Z., Zheng, Y., Qian, B., Zhong, Y., & Zhao, Y. (2014). Thermal behavior, microstructure and protein quality of squid fillets dried by far-infrared assisted heat pump drying. *Food Control, 36*(1), 102–110.

Gongnian, X., Min, Z., Weihua, D., Yanyang, X., Jincai, S., Yiping, C., & Jianshen, A. (2005). The invention relates to a preparation method of combined dehydrated fruits and vegetables by vacuum freeze drying and then hot air drying. *Chinese patent,* CN1711854A, 1–3.

Haonan, H. (2020). *Appearance quality control of jujube slices during drying based on glass transition theory*. Chinese Academy of Agricultural Sciences. Dissertation.

Hills, B. P., & Le Floc'h, G. (1994). NMR studies of non-freezing water in cellular plant tissue. *Food Chemistry, 51*(3), 331–336.

Hills, B. P., & Remigereau, B. (1997). NMR studies of changes in subcellular water compartmentation in parenchyma apple tissue during. *International Journal of Food Science & Technology, 32*, 51–61.

Hills, B. P., Takacs, S. F., & Belton, P. S. (1990). A new interpretation of proton NMR relaxation time measurements of water in food. *Food Chemistry., 37*(2), 95–111.

Honghong, D. (2012). *Studies on influencing factors of collapse phenomenon for freeze dried papasya slices*. Guangxi University.

Jianrong, C., Yue, L., Junwen, B., Li, S., & Hongwei, X. (2019). Three-dimensional imaging of morphological changes of potato slices during drying. *Transactions of the Chinese Society of Agricultural Engineering, 35*(1), 1–7.

Jingjing, Y., Jinfeng, B., & Yuanyuan, D. (2011). Effect of drying treatment methods on the quality properties of red jujube. *Modern Food Science and Technology, 27*(6), 610–614.

Karathanos, V. (1993). Collapse of structure during drying of celery. *Drying Technology, 11*(5), 1005–1023.

Koç, B., Eren, İ, & Kaymak Ertekin, F. (2008). Modelling bulk density, porosity and shrinkage of quince during drying: The effect of drying method. *Journal of Food Engineering, 85*(3), 340–349.

Lespinard, A. R., Bon, J., Cárcel, J. A., Benedito, J., & Mascheroni, R. H. (2014). Effect of ultrasonic-assisted blanching on size variation, heat transfer, and quality parameters of mushrooms. *Food and Bioprocess Technology, 8*(1), 41–53.

Lili, Z., Xiangyou, W., Zhongcai, W., & Chuanzhu, S. (2016). Structural properties research of infrared radiation drying for carrot slices. *Transactions of the Chinese Society for Agricultural Machinery, 47*(7), 6.

Lozano, J. E., Rotstein, E., & Urbicain, M. J. (1983). Shrinkage, porosity and bulk-density of foodstuffs at changing moisture contents. *Journal of Food Science, 48*, 1497–1553.

Lv, W., Zhang, M., Bhandari, B., Li, L., & Wang, Y. (2017). Smart NMR method of measurement of moisture content of vegetables during microwave vacuum drying. *Food and Bioprocess Technology, 10*(12), 2251–2260.

Macedo, L. L., Corrêa, J. L. G., da Silva Araújo, C., Vimercati, W. C., & Júnior, I. P. (2021). Convective drying with ethanol pretreatment of strawberry enriched with isomaltulose. *Food and Bioprocess Technology, 14*(11), 2046–2061.

Miaomiao, L., Luelue, H., & Xu, D. (2020). Quality change and moisture distribution of kiwifruit during FD-MVD. *Food and Fermentation Industries, 46*(15), 7.

Miaoqing, Z. (2019). *The influence of different dried method on Pleurotus eryngii quality*. Shanxi Agricultural University.

Nieto, A. B., Vicente, S., Hodara, K., Castro, M. A., & Alzamora, S. M. (2013). Osmotic dehydration of apple: Influence of sugar and water activity on tissue structure, rheological properties and water mobility. *Journal of Food Engineering, 119*(1), 104–114.

Pikal, M. J., & Shah, S. (1990). The collapse temperature in freeze drying: Dependence on measurement methodology and rate of

water removal from the glassy phase. *International Journal of Pharmaceutics, 62*(2–3), 165–186.

Polat, A., & Izli, N. (2022). Drying characteristics and quality evaluation of 'Ankara' pear dried by electrohydrodynamic-hot air (EHD) method. *Food Control, 134*, 108774.

Prothon, F., & Ahrné, L. (2003). Mechanisms and prevention of plant tissue collapse during dehydration: A critical review. *Critical Reviews in Food Science & Nutrition, 43*(4), 447–479.

Qinghui, W., Zhongxin, L., Shengkun, Y., & Lizi, B. (2017). Hot-air drying shrinkage characteristics and color changing of apricot. *Southwest China Journal of Agriculture, 30*(5), 1189–1193.

Su, D., Lv, W., Wang, Y., Wang, L., & Li, D. (2020). Influence of microwave hot-air flow rolling dry-blanching on microstructure, water migration and quality of Pleurotus eryngii during hot-air drying. *Food Control, 114*, 107228.

Sun, Q., Min, Z., Mujumdar, A. S., & Yang, P. (2019a). Combined LF-NMR and artificial intelligence for continuous real-time monitoring of carrot in microwave vacuum drying. *Food and Bioprocess Technology, 12*(8), 551–562.

Sun, Q., Zhang, M., & Mujumdar, A. S. (2019b). Recent developments of artificial intelligence in drying of fresh food: A review. *Critical Reviews in Food Science and Nutrition, 59*(14), 2258–2275.

Sun, Q., Zhang, M., & Yang, P. (2019c). Combination of LF-NMR and BP-ANN to monitor water states of typical fruits and vegetables during microwave vacuum drying. *Lwt, 116*, 108548.

Talens, C., Castro, M., & Fito, P. J. (2017). Effect of microwave power coupled with hot air drying on sorption isotherms and microstructure of orange peel. *Food and Bioprocess Technology, 11*(4), 723–734.

Vallespir, F., Crescenzo, L., Rodríguez, Ó., Marra, F., & Simal, S. (2019). Intensification of low-temperature drying of mushroom by means of power ultrasound: Effects on drying kinetics and quality parameters. *Food and Bioprocess Technology, 12*(5), 839–851.

Wang, D., Zhang, M., Wang, Y., & Martynenko, A. (2018a). Effect of pulsed-spouted bed microwave freeze drying on quality of apple cuboids. *Food and Bioprocess Technology, 11*(5), 941–952.

Wang, J., Law, C., Nema, P., Zhao, J., Liu, Z., Deng, L., Gao, Z., & Xiao, H. (2018b). Pulsed vacuum drying enhances drying kinetics and quality of lemon slices. *Journal of Food Engineering, 224*, 129–138.

Xueyuan, W., Kun, G., Qinqin, C., Jinfeng, B., Xinye, W., & Jianyong, Y. (2015). Water diffusion characteristics of apple slices during short and medium-wave infrared drying. *Transactions of the Chinese Society of Agricultural Engineering, 31*(12), 7.

Yue, L. (2020). *Study on the method of measuring the appearance quality of fruit and vegetable materials during drying*. Jiangsu University.

Yuyan, P., Zhenhua, D., & Jingni, Z. (2021). Analysis of internal moisture changes of persimmon slices during intermittent microwave drying using low-field NMR. *Science and Technology of Food Industry, 42*(14), 7.

Zeng, S., Wang, B., Lv, W., Wang, L., & Liao, X. (2022). Dynamic analysis of moisture, dielectric property and microstructure of ginger slices during microwave hot-air flow rolling drying. *Food Control, 134*, 108717.

Zhen, S. (2019). *Study on Pleurotus eryngii heat pump drying technology and non-destructive testing of moisture content in drying process*. Nanjing Agriculture University.

Zhengxiang, M. (2016). *The Pleurotus eryngii chips processing technology optimization research and product development*. Shandong Agriculture University.

Zhengyu, M., & Zhide, Z. (1996). *Principle and application of infrared radiation heating and drying*. China Machine Press.

Zielinska, M., Zielinska, D., & Markowski, M. (2017). The effect of microwave-vacuum pretreatment on the drying kinetics, color and the content of bioactive compounds in osmo-microwave-vacuum dried cranberries (Vaccinium macrocarpon). *Food and Bioprocess Technology., 11*(3), 585–602.

Zongbo, L. (2016). *Effect of far-infrared drying on characteristics and quality of Agaricus bisporus*. Northeast Forestry University.